

Chapter 44

Theoretical Modeling and Experimental Study of HIFU Transducers and Acoustic Fields

A.N. Rybyanets, A.A. Naumenko, N.A. Shvetsova, V.A. Khokhlova, O.A. Sapozhnikov and A.E. Berkovich

Abstract Recent advances in the fields of physical acoustics, imaging technologies, piezoelectric materials, and ultrasonic transducer design have led to emerging of novel methods and apparatus for ultrasonic diagnostics, therapy, and anesthetics as well as an expansion of traditional application fields. The chapter presents the results of theoretical modeling and experimental study of different High Intensity Focused Ultrasound (HIFU) transducers. Numerical solutions of parabolic Khokhlov-Zabolotskaya-Kuznetsov (KZK) equation were obtained for nonlinear focused fields. Technological peculiarities of the HIFU transducer design as well as theoretical and numerical models of such transducers and the corresponding HIFU fields are discussed. Several HIFU transducers of different design have been fabricated using different advanced piezoelectric materials. Acoustic field measurements for those transducers have been performed using a calibrated fiber optic hydrophone and an ultrasonic measurement system. The results of theoretical modeling and ex vivo experiments with different tissues (fresh porcine mussels, adipose tissue and bovine liver), as well as in vivo experiments with blood vessels are present that prove the efficacy, safety and selectivity of the developed HIFU transducers and methods.

A.N. Rybyanets (✉) · A.A. Naumenko · N.A. Shvetsova
Institute of Physics, Southern Federal University, 194, Stachki Ave.,
344090 Rostov on Don, Russia
e-mail: arybyanets@gmail.com

V.A. Khokhlova · O.A. Sapozhnikov
Physics Faculty, Moscow State University, Leninskie Gory, 119991 Moscow, Russia

A.E. Berkovich
Sankt-Petersburg Politechnical University, 29, Polytechnicheskaya Str.,
195251 Sankt-Petersburg, Russia

44.1 Introduction

Ultrasound has found usage in all aspects of the medical field, including diagnostic, therapeutic, and surgical applications. The use of ultrasound as a valuable diagnostic and therapeutic tool in several fields of clinical medicine is now so well established that it can be considered essential for good patient care [1]. However, remarkable advances in ultrasound imaging technology over last decade have permitted us now to envision the combined use of ultrasound both for imaging/diagnostics and for therapy. Therapeutic ultrasound has been in use for many years [1–4]. Early applications were those for which tissue heating was the goal, and so it was used to treat soft tissue injuries such as may be incurred during sport activities. More recently, attention has been drawn both to high intensity focused beams that may be used for thermal ablation of selected regions and also to low intensity fields that appear to be able to stimulate physiological processes, such as tissue repair, without biologically significant temperature rises. Ultrasonic tools are used for therapeutic effect in dentistry and are being investigated for use in thrombolysis.

Ultrasound beyond the diagnostic ranges can initiate various kinds of effects when insonated into biological tissue. The ability of ultrasound to interact with tissue to produce biological changes has been known for a long time [3]. Much of the early drive to understand these interactions came from an interest in harnessing ultrasonically induced changes for therapeutic benefit. More recently, the concern has been to understand any possible hazard that may arise from diagnostic ultrasound imaging. It is convenient to divide therapeutic ultrasound into two classes, i.e. applications that utilize ‘low’ ($0.125\text{--}3\text{ W/cm}^2$) and ‘high’ intensities ($\geq 5\text{ W/cm}^2$). The intention of the low intensity treatments is to stimulate normal physiological responses to injury or to accelerate some processes such as the transport of drugs across the skin. The purpose of the high intensity treatments is rather to selectively destroy tissue in a controlled fashion. The resulting effects include thermal, mechanical, chemical, and optical reactions. Mechanical effects, more specifically, may consist of acoustic cavitation, radiation force, shear stress, and acoustic streaming/microstreaming. Among them, the thermal effect and acoustic cavitation are the most significant, and their mechanisms of action have been relatively well-understood [1, 2]. It is however often extremely difficult to identify positively the mechanisms involved in producing biological change, and indeed to isolate non-thermal effects from the thermal ones.

The thermal effect is caused by the absorption of ultrasound in biological tissue. Ultrasonic waves cause vibration or rotation of molecules or part of macromolecules in tissue, and this movement results in frictional heat. Depending on the temperature and the duration of contact, the tissue may become more susceptible to chemotherapy or radiotherapy ($>43\text{ }^\circ\text{C}$, 1 h) or alternatively, protein denaturation may occur (coagulation necrosis) ($56\text{ }^\circ\text{C}$, 1 s) [1, 2, 5]. Beneficial effects that arise from ultrasonically induced heating include an increase in extensibility of collagenous structures such as tendons and scar tissue, a decrease in joint stiffness,

pain relief, changes in blood flow, decrease in muscle spasm, and, at high intensities, selective tissue ablation as achieved in focused ultrasound surgery [4].

Excluding the effects of thermal transfer, the temperature elevation in biological tissue induced by ultrasound (plane wave) absorption is theoretically linearly proportional to acoustic intensity in the following manner ($\partial T/\partial t = 2\alpha I/\rho C_p = 0.014I$, where T is the temperature ($^{\circ}\text{C}$), t is the time (s), α is a absorption coefficient $\approx 0.03 \text{ Np/cm}$ in tissue-like medium at 1 MHz, I = acoustic intensity, ρ is the density $\approx 1 \text{ g/cm}^3$ in tissue-like medium, C_p is the specific heat $\approx 4.2 \text{ J/(g } ^{\circ}\text{C)}$ in tissue-like medium) [6, 7]. Because of this linearity and predictability, a thermal effect was traditionally preferred to a mechanical effect in the medical applications of unfocused and focused ultrasound.

Non-thermal mechanisms that can produce beneficial (therapeutic) changes in tissue may be cyclic or non-cyclic in nature. The early literature refers to “micro-massage” [8]. This is presumably thought to be an effect due to the periodic nature of the sound pressure field. The one of non-cyclic effect thought to be involved in ultrasound therapy is acoustic streaming. This may be due to stable, oscillating cavities, or to radiation forces in intra- or extracellular fluids. Streaming may act to modify the local environment of a cell leading, for example, to alter concentration gradients near of an extracellular membrane. The concentration gradient affects the diffusion of ions and molecules across a membrane, and thus streaming may account for the reported changes in the potassium and calcium content of cells following ultrasonic exposure [1].

Acoustic cavitation, defined as the formation and activity of a gas- or vapor-filled cavity (bubble) in a medium exposed to ultrasound, plays a major role in the mechanical effects and minor roles in the chemical and the optical effects of ultrasound medical technology. If biological tissue is insonated by an ultrasound wave, more intense than a specific threshold, negative pressure representing the rarefaction of the wave, may be large enough to draw gas out of the tissue solution to form a bubble. It is easy to understand the underlying mechanism if it is compared to the numerous bubbles formed by vigorous rotation of a motorboat screw. This bubble either repeats radial oscillations being in a resonant size with the ultrasound frequency (stable cavitation; non-inertial cavitation) or oscillates in a similar manner expanding gradually above its resonant size due to net influxes of gas and vapor into the bubble (rectified diffusion), and finally disintegrates by a violent and asymmetrical collapse (unstable cavitation; inertial cavitation) [1, 9]. Acoustic cavitation, particularly inertial cavitation, can cause a significant degree of mechanical and thermal effects as well as chemical and optical effects. The thermal effect caused by acoustic cavitation is larger than that caused by ultrasound absorption alone. Mechanical and thermal effects by acoustic cavitation are generally known to be complex, unpredictable, and, sometimes, detrimental. The threshold of acoustic cavitation depends on the (negative) pressure amplitude, ultrasound frequency, and the tissue where cavitation occurs [1, 8, 10].

Radiation force is a force exerted at an interface between two media or inhomogeneity in a medium due to the passage of ultrasound waves. An acoustic field in fluid may set up acoustic streaming; the transfer of momentum to liquid, by the absorption of energy from an acoustic field, causes acoustic streaming. The fluid velocity caused by acoustic streaming is spatially non-uniform thereby generating a velocity gradient in the field. This gradient causes shear stress. Acoustic streaming caused by an oscillating bubble in a sound field immediately surrounding the bubbles is specifically referred to as acoustic microstreaming. Shear stress formed by microstreaming is an important mechanism underlying many biological reactions [1, 10].

Traditional therapeutic applications of ultrasound include the treatment of soft tissue and bone injuries, wound healing, hyperthermic cancer treatment, focused ultrasound surgery of Parkinson's disease, glaucoma and retinal detachment and for sealing traumatic capsular tears, benign prostatic hyperplasia, the liver, the kidney, prostate and bladder tumours, vascular occlusion therapy, and tool surgery [1–5]. Most physiotherapy units offer spatial average intensities up to 3 W/cm^2 and offer one or more transducers operating at discrete frequencies in the range of 0.75–5 MHz. The choice of transducer depends on the depth of the target to be treated, deeper targets require lower frequencies because of the frequency dependence of ultrasonic attenuation. Devices offer either discrete intensity settings or continuously variable controls. The output may be continuous or pulsed. Pulsed exposures are often chosen when thermal effects are to be kept to a minimum. Commonly available pulsing regimes are 2:2 and 2:8 ms [1].

Therapeutic transducers are usually made of low loss lead zirconate-titanate (PZT) or recently from porous ceramics and piezocomposites [11–13]. In the past decade, with the advent of faster processing, specialized contrast agents, understanding of nonlinear wave propagation, novel real-time signal and image processing as well as new piezoelectric materials, processing technologies and ultrasound transducer designs and manufacturing, ultrasound imaging and therapy have enjoyed a multitude of new features and clinical applications [14, 15].

The chapter presents the results on development and experimental study of different high intensity focused ultrasound (HIFU) transducers. Technological peculiarities of the HIFU transducer design as well as theoretical and numerical models of such transducers and the corresponding HIFU fields are discussed. Several HIFU transducers of different design have been fabricated using different advanced piezoelectric materials. Acoustic field measurements for those transducers have been performed using a calibrated fiber optic hydrophone and an ultrasonic measurement system (UMS). The results of *ex vivo* experiments with different tissues as well as *in vivo* experiments with blood vessels are present that prove the efficacy, safety and selectivity of the developed HIFU transducers and methods.

44.2 Theoretical Calculations and Numerical Modeling of HIFU

The characterization of medical acoustic devices that operate at high output levels has been a research topic and an issue of practical concern for several decades [1, 2]. The importance of nonlinear effects has been considered and addressed even at diagnostic levels of ultrasound [16]. In lithotripsy and HIFU, these effects are critical as acoustic pressures of up to 100 MPa or higher can be reached; such pressures are two or even three orders higher in magnitude than diagnostic ultrasound.

Numerical modeling has been used to predict high amplitude acoustic fields from medical devices. One advantage of modeling is that it can be used to determine the acoustic field in both water and tissue. Numerical algorithms, most commonly based on the nonlinear parabolic Khokhlov-Zabolotskaya-Kuznetsov (KZK) equation, have been developed and applied to the nonlinear fields of lithotripters, unfocused ultrasonic piston sources, diagnostic ultrasonic transducers operating in tissue harmonic imaging mode [17], focused ultrasound sources [18], and HIFU sources [16, 19].

For strongly focused fields non-linear models such as Westervelt equation can be used, which is a generalization of the classical wave equation to the nonlinear case in the approximation of the absence of back propagating waves. Even more complex models based on the solution of the full nonlinear wave equation have been developed [7]. However, these approaches require large computing power and time-consuming calculations (up to several days) on supercomputers, i.e. practically inapplicable to practical problems. This difficulty can be significantly reduced by using the evolution equation for the quasi-plane wave. The corresponding equation in nonlinear acoustics equation is known as the KZK equation [6, 7].

44.2.1 Theoretical Calculation of HIFU Fields

As is known, the system of hydrodynamic equations in the general case cannot be solved analytically, and the basic approach is to use numerical simulation. It is possible to solve numerically the complete system of hydrodynamic equations, but in practice, it is usually unrealizable because of limitations on available computer memory and its computational speed even using the modern computing clusters. However, one can find reasonably accurate solution to the practical problem of interest with some simplifying assumptions.

It is often assumed that the amplitude of acoustic waves is sufficiently low so that the ultrasound field can be described in approximation of linear acoustic. In the linear case we can reduce the problem to considering harmonic (sinusoidal) waves: $p(\mathbf{r}, t) = P(\mathbf{r}) \exp(-i\omega t)/2 + P^*(\mathbf{r}) \exp(i\omega t)/2$, where p is the acoustic pressure, P is its complex amplitude, ω is the angular frequency. The corresponding equation

for harmonic waves in homogeneous medium is the Helmholtz equation: $\Delta P + (\omega^2/c_0^2)P = 0$, where c_0 is the sound speed in the medium. The solution of this equation for one-way propagation from ultrasound transducer can be written as [17]:

$$P(\mathbf{r}) = -i\rho_0 c_0 \frac{k}{2\pi} \int_S \frac{V(\mathbf{r}') e^{ik|\mathbf{r}-\mathbf{r}'|}}{|\mathbf{r}-\mathbf{r}'|} dS' \quad (44.1)$$

This expression is called the Rayleigh integral.

Rayleigh integral can be used for the calculation of acoustic field generated by the source in the shape of a spherical cap under the assumption that the focusing angle is small and the radius of curvature of the radiating surface is much larger than the wavelength [17]. Then locally the surface elements radiate as a flat source, and it can be assumed that the resulting field given by the (44.1) is sufficiently accurate. With a uniform velocity distribution on the cap one can obtain a simple analytical expression for the amplitude of the pressure on the axis of the transducer:

$$P = P_0 \frac{e^{ikz} - e^{ikR_{\max}}}{1 - z/F}, \quad (44.2)$$

where z is the axial coordinate, R_{\max} is the distance from the observation point to the edge of the transducer, P is the complex amplitude of the acoustic pressure on the axis of the transducer (at the point with coordinate z , measured from the center of the bowl), F is the radius of curvature of the bowl, $P_0 = \rho_0 c_0 V$ is the characteristic acoustic pressure on the surface of the transducer, V is the amplitude of the normal velocity component of the radiating surface. The distance $R_{\max} = R_{\max}(z)$ can be written as follows:

$$R_{\max} = F \sqrt{1 + \left(1 - \frac{z}{F}\right)^2 - 2\left(1 - \frac{z}{F}\right) \cos \alpha}, \quad (44.3)$$

where α is the half-opening angle of the cap, i.e. the angle between the rays directed from the geometrical focus ($z = F$) to the center of the bowl and to its edge.

The above result for the sources in the form of a spherical cap can be simply extended to the case of a source in the form of an annular spherical segment. Indeed, since the problem is linear, we can embed in a spherical cap another coaxial one (with the same curvature, but different diameter). Then it is possible to obtain oscillation only of an annular spherical segment if excite the surface of the above mentioned cap in antiphase. Consequently, due to the principle of superposition, the field of the ring can be obtained by subtracting fields of two caps of different diameters.

Therefore, if the center of the transducer has a hole, then the solution will be:

$$p(z, t) = \frac{p_0 e^{-i\omega t}}{1 - z/F} (e^{ikR_{\min}} - e^{ikR_{\max}}), \quad A(z) = \frac{2p_0}{1 - z/F} \left| \sin \left(k \frac{R_{\min} - R_{\max}}{2} \right) \right|, \quad (44.4)$$

where $R_{\min} = F \sqrt{1 + (1 - z/F)^2 - 2(1 - z/F) \cos \beta_1}$, $\sin \beta_1 = a_1/F$.

If the beam propagates in absorbing medium, then attenuation for the pressure amplitude $A(z)$ of the source with a hole can be taken into account as follows:

$$A(z) = \left| \frac{2p_0}{1 - z/F} \sin \left(k \frac{R_{\min} - R_{\max}}{2} \right) \right| \exp(-\alpha z), \quad (44.5)$$

where α is the attenuation at the frequency of the radiation.

For the calculation of the medium heating one can use a standard formula: $Q = 2\alpha I$.

The frequency dependence of the attenuation α , obtained experimentally for a number of liquids and tissues, can be found in [1].

Since the regime of high intensities is required for stopping the bleeding, non-linear propagation of acoustic waves occurs, and theoretical description requires more complex models than for the case of low intensity.

For strongly focused fields, non-linear models such as Westervelt equation can be used, which is a generalization of the classical wave equation to the nonlinear case in the approximation of the absence of back propagating waves [16]. Even more complex models based on the solution of the full nonlinear wave equation have been developed [5, 6]. However, these approaches require large computing power and time-consuming calculations (up to several days) on supercomputers, i.e. practically inapplicable to practical problems. This difficulty can be significantly reduced by using the evolution equation for the quasi-plane wave. The corresponding equation in nonlinear acoustics equation is known as the KZK equation [16].

44.2.2 Numerical Modeling

Numerical modeling of experimental conditions was performed using a KZK-type nonlinear parabolic equation generalized for the frequency-dependent absorption properties of the propagation medium:

$$\frac{\partial}{\partial \tau} \left[\frac{\partial p}{\partial z} - \frac{\beta}{\rho_0 c_0^3} p \frac{\partial p}{\partial \tau} - L_{abs}(p) \right] = \frac{c_0}{2} \Delta_{\perp} p, \quad (44.6)$$

where p is the acoustic pressure, z is the propagation coordinate along the axis of the beam, $\tau = t - z/c_0$ is the retarded time, c_0 is the ambient sound speed, p_0 is the ambient density of the medium, β is a coefficient of nonlinearity, Δ_{\perp} is the Laplacian with respect to the transverse coordinate r , and L_{abs} is the linear operator that accounts for the absorption and dispersion of the medium.

For simulations in water, thermoviscous absorption was included as

$$L_{abs} = \frac{b}{2\rho_0 c_0^3} \frac{\partial^2 p}{\partial \tau^2} \quad (44.7)$$

where b is the dissipative parameter of water. For simulations in gel, the propagation path for ultrasound comprised a two-layer medium consisting of water followed by tissue-mimicking gel phantom. The frequency-dependent absorption of ultrasound in the gel was included in the model according to a nearly linear power law combined with weak thermoviscous absorption, as in the water:

$$\alpha(f) = \frac{2\pi^2 f^2 b}{\rho_0 c_0^3} + \alpha_0 \left(\frac{f}{f_0} \right)^{\eta} \quad (44.8)$$

Here α_0 is the absorption parameter of the gel at the fundamental frequency f_0 , and variation of the sound speed with frequency was calculated for the power law term (η) in (44.8) using the local dispersion relations.

The boundary condition for (44.6) was set by translating the pressure amplitude, p_0 , uniformly distributed over the curved surface of the source to the plane $z = 0$. The translation of the amplitude was performed using a geometrical acoustics approximation following the spherical convergence of the field. The focusing phase shift along the radial coordinate was introduced in the parabolic approximation as

$$p(z = 0, r, \tau) = \frac{p_0}{\sqrt{1 + r_0^2/F^2}} \sin\left(2\pi f_0 \left(\tau + \frac{r^2}{2c_0 F}\right)\right), \quad (44.9)$$

if $r < r_0/\sqrt{(1 + r_0^2/F^2)}$ and $p(z = 0, r, \tau) = 0$, elsewhere. Here, $2r_0$ is the aperture of the source and F is its radius of curvature.

Equation (44.6) was solved numerically in the frequency domain using a previously developed finite difference algorithm. The acoustic pressure waveform was represent as a Fourier series expansion as

$$p(z, r, \tau) = \sum_{n=1}^{\infty} c_n(z, r) e^{in2\pi f_0 \tau}, \quad (44.10)$$

where c_n is the complex amplitude of the n th harmonic. A set of nonlinear-coupled differential equations for the amplitudes of the harmonics was derived and integrated numerically using the method of fractional steps and an operator-splitting

procedure. The simulations were performed assuming radial symmetry of the HIFU source.

To characterize the HIFU output level in the focal zone in water or in gel, two values of the spatial peak intensity were introduced. These values will be referred to in the chapter as focal intensities. The first value, I_N , was calculated from the numerically modeled nonlinear waveform as a combination of the focal intensities of all harmonic components:

$$I_N = f_0 \int_0^{1/f_0} \frac{p^2}{\rho_0 c_0} d\tau = \frac{2}{\rho_0 c_0} \sum_{n=1}^{\infty} |c_n|^2. \quad (44.11)$$

The second value, I_L , was calculated based on the results of the linear acoustic propagation modeling as

$$I_L = \frac{P_F^2}{2\rho_0 c_0}, \quad (44.12)$$

where p_F is the focal (i.e., spatial peak) pressure amplitude in situ. The linear focusing gain of the source was defined as a ratio of the focal and source pressure amplitude obtained from linear modeling in water:

$$G = p_F/p_0. \quad (44.13)$$

The medium heating was calculated as follows:

$$Q = \sum_{n=1}^{\infty} 2\alpha_n I_n, \quad (44.14)$$

where $\alpha_n = \alpha(n\omega_0)$ is the attenuation of n th harmonic and $I_n = |C_n|^2 / (2\rho_0 c_0)$ is the intensity of this harmonic. Thus, total heat source in the non-harmonic (in particular, in non-linear) wave is the sum of the heat sources of the individual harmonics, and each harmonic absorption may be considered in the plane wave approximation.

44.3 Applications of HIFU for Hemostasis, Thrombolysis and Ablation

Acoustic hemostasis may provide an effective method in surgery and prehospital settings for treating trauma and elective surgery patients. Application of HIFU therapy to hemostasis was primarily initiated in an attempt to control battlefield injuries on the spot. High-intensity ultrasound ($ISA = 500\text{--}3000 \text{ W/cm}^2$) is usually

adopted for hemostasis. Many studies on animal models have been successful for both solid organ and vascular injuries [1]. The thermal effect has a major role in hemostasis. The proposed mechanisms of its action are as follows. Structural deformation of the parenchyma of a solid organ due to high temperature induces a collapse of small vessels and sinusoids or sinusoid-like structures. Heat also causes coagulation of the adventitia of vessels, and subsequently, fibrin-plug formation. The mechanical effect of acoustic cavitation also appears to play a minor role in hemostasis. Microstreaming induces very fine structural disruption of the parenchyma to form a tissue homogenate that acts as a seal and induces the release of coagulation factors. No statistically significant hemolysis or changes in the number of white blood cells and platelets have been observed when blood is exposed to HIFU with intensities up to 2000 W/cm^2 . The main drawback of the hemostasis applications is low ultrasound absorption ability of blood and, as a result, low heating and coagulation rate at real blood flow. In this section, HIFU transducer design, nonlinear acoustic field calculations and *in vivo* experiments on blood vessels confirming enhanced hemostasis are described.

Ultrasound can play a significant role in thrombolysis. Ultrasound with/without a thrombolytic agent has been shown to be effective in enhancing thrombolysis. Thrombolysis is achieved with low intensity US ($\text{ISA} = 0.5\text{--}1 \text{ W/cm}^2$) and is known to be associated with non-thermal mechanisms [1–3]. Microstreaming by acoustic cavitation produces a strong mechanical force around the cell membranes that causes the pores or channels to open. This increases the bioavailability of thrombolytic agents on the surface of a thrombus. The radiation force of the ultrasound itself could push the drug to the lesion (“push effect”). The direct mechanical effect with/without microstreaming could cause alterations to the fibrin mesh. These effects, described above, are believed to work synergistically to cause thrombolysis [2]. There are two methods of delivering ultrasound to thrombosed vessels. One is an extracorporeal approach. This is noninvasive, but requires higher ultrasound energy for compensating attenuation through an intervening tissue; in addition, it may have the potential risks of complications and treatment-failure due to the intervening tissues. Clinical trials using the extracorporeal low frequency ultrasound (as in transcranial Doppler ultrasound) for brain ischemia with the assistance of a tissue plasminogen activator have turned out to be successful [3]. The other method is via a miniaturized transducer, at the tip of an arterial catheter, from which a thrombolytic drug releases. This system is minimally invasive and commercially available [3].

Focused ultrasound surgery (FUS) is used for local ablation therapy of various types of tumors using HIFU ($\text{ISA} = 100\text{--}10,000 \text{ W/cm}^2$). The two main mechanisms involved in FUS are thermal effects by ultrasound absorption and mechanical effects involving thermal effects in part, induced by acoustic cavitation. The thermal effect by absorption has been traditionally employed because it is relatively accurately predictable and thus easy to control. This enables the therapy to be safe even though thermal ablation by the conventional method of FUS generally requires a long surgical time for clinical practice. The effects of cavitation have proven to have potential in improving the efficiency of the therapy by enlarging the ablation size

and subsequently reducing the procedure-time for ablation [3]. However, these advantages could be accompanied by a longer cooling time and a relatively high risk of complication.

The shape of a classical thermal lesion resembles a cigar, paralleling the direction of the ultrasound propagation, measuring about 1.5–2 mm in width and about 1.5–2 cm in length when produced by a typical clinical 1.5 MHz HIFU field [3, 8, 9]. This single thermal lesion is extremely small in comparison to the sizes of common clinical tumors. The individual thermal lesions are stacked up closely without leaving intervening viable tissue to form a sufficient ablation zone to cover the tumor itself as well as the safety margin. The tissue-homogeneity influences the shapes of the thermal lesion while the tissue-perfusion may affect its size. The frequency of ultrasound is adjusted to optimize surgical conditions, keeping sonic attenuation low (advantage of low frequency) as well as making energy focused sharply enough (advantage of high frequency) [3].

The histological changes made by FUS have been investigated. Thermal damage after ultrasound absorption has been described as an “island and moat” in which the “island” represents an area of complete coagulation necrosis and complete destruction of the tumor-supplying vessels whereas the “moat” refers to the surrounding rim-like area that is 6–10 cells-thick and composed of glycogen-poor cells (2 h) that usually die within 48 h. Later, granulation tissue, fibroblast infiltrates and finally retraction/scar formation occurs [1, 2]. The changes that occur because of acoustic cavitation are both coagulation necrosis and mechanical tearing. Mechanical tearing, which is attributed to tissue boiling as well as the mechanical effects of acoustic cavitation, manifests as holes or implosion cysts upon microscopic examination [3].

44.4 Limitations and Future Works

Major differences of HIFU therapy from other interventional therapeutic modalities are its complete non-invasiveness and sharp, tailorable treatment margins, which may lead to treatments with very low complication rates. However, several complications have been known to occur after HIFU therapy. These are mostly due to high-energy ultrasonic waves reflected on gas or bony structures [1, 2]. Skin-burn can be caused by poor acoustic coupling between the skin and the therapeutic window (e.g. poor shaving) or a previous operation scar. In cases of liver treatment, reflected ultrasonic waves on ribs can induce overlying soft tissue damage including the skin. Gas-containing bowel loops act in the same manner and can cause thermal injury of the bowel wall. Sciatic nerve injury was also reported after HIFU therapy for uterine leiomyoma. This complication is deemed to be caused either directly by high-energy ultrasonic waves that pass the focal therapeutic zone or indirectly by elevated temperatures of the pelvic bone. If the focal zone locates superficially as in case of breast cancer, direct thermal injury of overlying skin can occur [2]. Likewise, internal organs just anterior or posterior to the focal zone could be

injured. In addition to these complications, HIFU therapy at the time of writing this manuscript, has displayed several other limitations, which are hampering the effective use of this modality in clinical practice. These include a long procedure time, difficulty in targeting and monitoring moving organs, sonic shadowing by bones or gas in bowels, and the relatively high cost of this technique in relation to its effectiveness and limitations.

Main limitation of HIFU for body shaping application (fat reduction, cellulite therapy) is a small size of focal zones and a small thickness of target tissues along with its spatial extension, leading to long procedure time, pain and injury of bones and vital organs.

However, recent technological advances are expected to resolve these problems. One example is the new MR-assisted HIFU device under development, which adopts the technique of an automatic on-line, spatiotemporal temperature control using a multispiral trajectory of the focal point and proportional, integral and derivative principles [2]. This system claims to be able to make a thermal lesion faster and more stably under real-time thermal monitoring even in moving organs than the existing devices [1].

In the field of body aesthetic applications, uses of new HIFU technologies (dynamical focusing and natural harmonics methods) in combination with other therapeutic and diagnostic modalities such as ultrasonic standing waves therapy, shear waves elasticity imaging and therapy, targeted drug/gene-delivery and combinational treatments (ultrasound—RF—vacuum massage), can be anticipated and has a more revolutionary clinical impact [3, 17, 18].

44.5 HIFU Transducers Design

HIFU transducer comprised 1.6 MHz spherical element made from porous piezoceramics [11, 12, 18] with 80 mm aperture and 40 mm centre hole having radius of curvature 54 mm. The piezoelement was sealed in custom-designed cylindrical housing filled with the mineral oil providing acoustic contact and cooling of the element. The housing had an acoustic window made of very thin (0.15 mm) PVC membrane. Centre opening was reserved for ultrasonic imaging transducer (Fig. 44.1).

44.6 Acoustic Field Calculations

Calculations of acoustic fields of HIFU transducers were made using the models and algorithms described above.

Figure 44.2 shows two-dimensional distributions of acoustic intensity in HIFU transducer's acoustic axis plane. Intensity levels are represent in absolute values (kW/cm^2). Calculations were made for two frequencies 1.6 MHz (a) and 2 MHz (b), respectively.

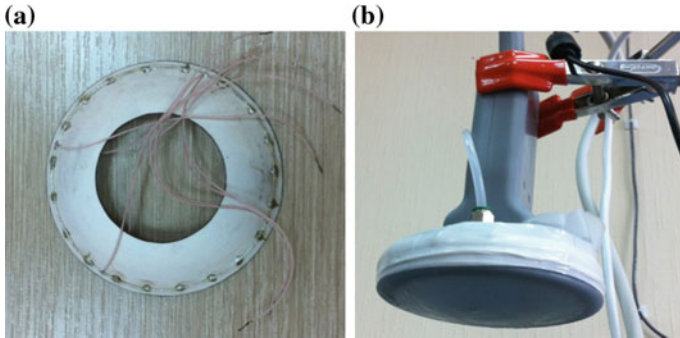


Fig. 44.1 Focusing piezoelement (a) and assembled HIFU ultrasonic transducer (b)

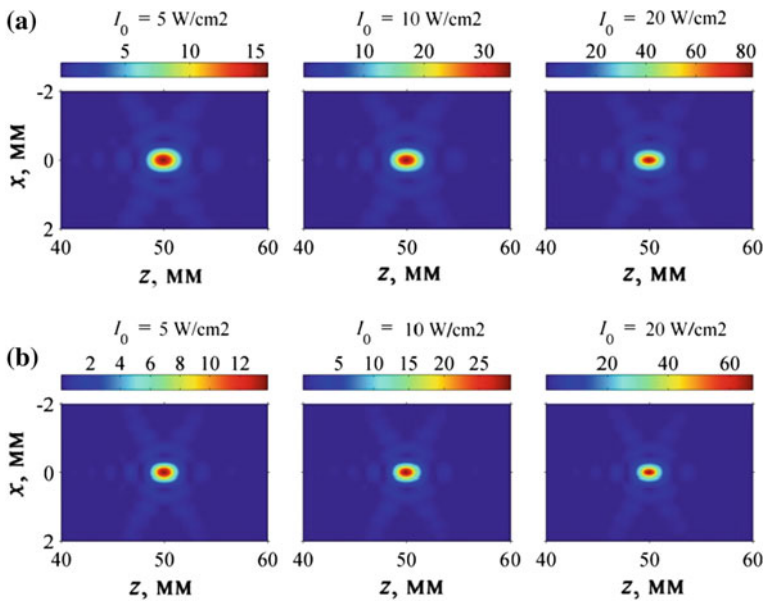


Fig. 44.2 Two-dimensional distributions of acoustic intensity in acoustic axis plane of HIFU transducer for 1.6 MHz (a) and 2 MHz (b) frequencies

Figure 44.3 shows two-dimensional distributions of heat sources power in HIFU transducer’s acoustic axis plane. Power density levels are represent in absolute values (kW/cm^3).

In Fig. 44.4, acoustic pressure signals in the focus, calculated at different initial intensities for 1.6 and 2 MHz, are shown. It is obvious that even at initial intensity level of $5 \text{ W}/\text{cm}^2$, nonlinear effects lead to pressure profile asymmetry that transforms to a shock front in focus at initial intensity $20 \text{ W}/\text{cm}^2$ that give rise to extreme heating.

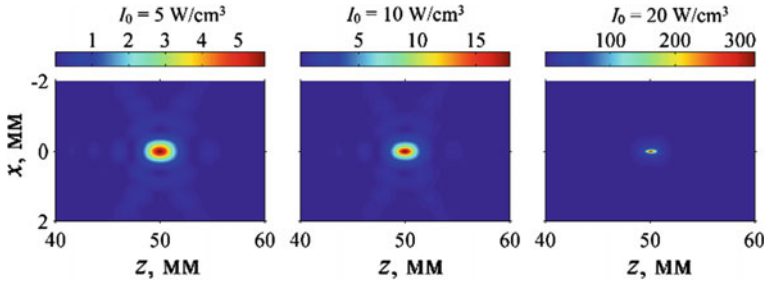


Fig. 44.3 Two-dimensional distributions of heat sources power in acoustic axis plane of HIFU transducer for 1.6 MHz frequency

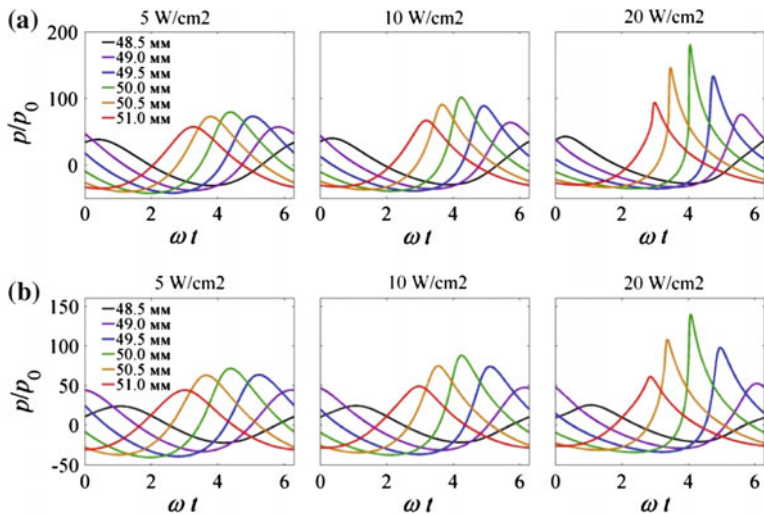


Fig. 44.4 Acoustic pressure signals in the focus calculated at different initial intensities for 1.6 MHz (a) and 2 MHz (b) frequencies

44.7 Ex Vivo Experiments on Tissues

Fresh porcine liver, muscle and adipose tissues were obtained from a butcher within 24 h of slaughter. A single element spherical PZT transducer (1.6 MHz, 80 mm aperture and 40 mm centre hole) has been used for experiments. The acoustic intensity for porous PZT transducer was 750 W/cm^2 (ISAL). The samples were placed in an oil bath and positioned right under the transducer such that focal point was placed inside the sample. The samples were irradiated by the harmonics frequency HIFU for 3–20 s at different duty cycles (from 1/2 to 1/100) and burst lengths (from 10 to 200 cycles) of the signals. After exposure the samples were sectioned along the beam axis respectively to compare the dimensions of the lesions [8, 9].

The photographs of thermal and cavitation lesions in the muscle, liver and porcine samples induced by HIFU are shown in Fig. 44.5.

44.8 In Vivo Experiments on Blood Vessels

The experiments were made on lamb's femoral artery at a standard protocol. During ultrasound exposure, arterial blood flow was temporarily stopped using intravascular balloon. Ultrasonic transducer with 1.6 MHz frequency described in previous sections was used for experiments. All acoustic measurements were performed in 3D Scanning System (UMS3) using a fiber-optic hydrophone (FOPH 2000) from Precision Acoustics Ltd. Waveforms from the hydrophones and the driving voltage were recorded using a digital oscilloscope LeCroy. The transducer was driven by a function generator Agilent 33521B and a linear rf-amplifier E&I model 2400L RF and operates in a CW mode. The acoustic intensity in the focal plane measured in water tank at 5000 W/cm^2 (I_{SAL}) was kept for the object treatment [18–21]. After sonication procedure and angiography study, the samples of femoral artery were extracted to confirm hemostasis and disclose vessel thrombus. The X-ray image of blood vessels obtained using contrast agents and photograph of dissected femoral artery are shown In Fig. 44.6.

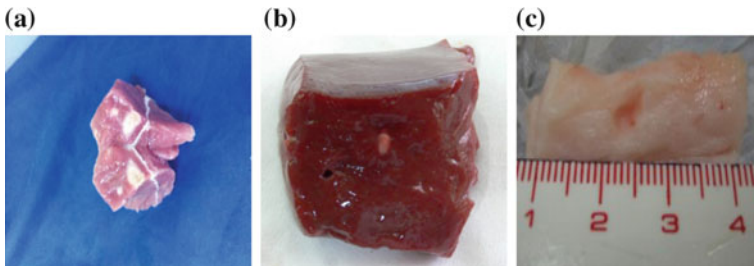


Fig. 44.5 Thermal (a, b) and cavitation (c) lesions in the muscle, liver and porcine samples induced by HIFU transducers. Treatment parameters: **a** CW—exposure time = 3 and 9 s, **b** CW—exposure time = 3 s, **c** burst mode—duty cycle = 1/20, burst length = 10 cycles, exposure time = 9 s

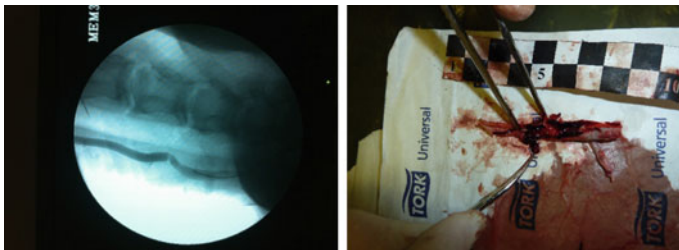


Fig. 44.6 Angiography image of blood vessels showing ultrasound hemostasis and photograph of vessel thrombus in dissected femoral artery

44.9 Conclusions

The results of theoretical modeling and experimental study of different HIFU transducers were presented. Ex vivo experiments in tissues (fresh porcine adipose tissue, bovine liver) and in vivo experiments in lamb's femoral artery were carried out using different protocols. The results of theoretical modeling and tissue experiments prove the efficacy, safety, and selectivity of the developed HIFU transducers and methods enhancing the tissue lysis and hemostasis and can be used for various therapeutic, surgical and cosmetic applications.

We have demonstrated that HIFU can be used to stop active bleeding from vascular injuries including punctures and lacerations. Using HIFU transducers, operated at a frequency of 1 or 2 MHz in continuous mode with intensities of 2000–5000 W/cm², we were able to stop bleeding from major blood vessels that were punctured with an 18- or a 14-gauge needle. Postponed hemostasis was observed at lamb's femoral artery experiments for all HIFU treatments. We have demonstrated that HIFU can be used to stop active bleeding from vascular injuries including punctures and lacerations. Those methods and transducers can be used also for various therapeutic, surgical and cosmetic applications.

Acknowledgments Work supported by the Russian Science Foundation (Grant No. 15-12-00023).

References

1. C.R. Hill, J.C. Bamber G.R. ter Haar (eds.), *Physical Principles of Medical Ultrasonics*, 2nd edn. (Wiley, 2004)
2. G.R. ter Haar, *Prog. Biophys. Mol. Biol.* **93**, 111 (2007)
3. A.N. Rybyanets, in *Piezoelectrics and Related Materials: Investigations and Applications*, Chap. 5, eds. by I.A. Parinov (Nova Science Publishers Inc., New York, 2012), p. 143
4. W. Summer, M.K. Patrick, *Ultrasonic Therapy—a textbook for physiotherapists* (Elsevier, London, 1964)
5. M. Dyson, M. Brookes, in *Ultrasound*, eds. by R.A. Lerski, P. Morley (Pergamon, Oxford, 1983), p. 61
6. V. Khokhlova, A. Ponomarev, M. Averkiou, L. Crum, *Acoust. Phys.* **52**, 481 (2006)
7. V.A. Khokhlova, R. Souchon, J. Tavakkoli, O.A. Sapozhnikov, D. Cathignol, *J. Acoust. Soc. Am.* **110**, 95 (2001)
8. A.N. Rybyanets, *AIP Conf. Proc.* **1215**, 287 (2010)
9. A.N. Rybyanets, M.A. Lugovaya, A.A. Rybyanets, *AIP Conf. Proc.* **1215**, 291 (2010)
10. A.P. Sarvazyan, L. Fillinger, L.R. Gavrilov, *Acoust. Phys.* **55**, 630 (2009)
11. A.N. Rybyanets, *IEEE Trans. UFFC* **58**, 1492 (2011)
12. A.N. Rybyanets, in *Piezoceramic Materials and Devices*, Chap. 3, eds. by I.A. Parinov (Nova Science Publishers Inc, New York, 2010), p. 113
13. A.N. Rybyanets, A.A. Rybyanets, *IEEE Trans. UFFC* **58**, 1757 (2011)
14. M. Fink, G. Montaldo, M. Tanter, *Ann. Rev. Biomed. Eng.* **5**, 465 (2003)
15. A.P. Sarvazyan, *Acoust. Soc. Am.* **123**, 3429 (2008)
16. V.G. Andreev, V.N. Dmitriev, Y.A. Pishchal'nikov, O.V. Rudenko, O.A. Sapozhnikov, A. P. Sarvazyan, *Acoust. Phys.* **43**, 123 (1997)

17. A.N. Rybyanets, V.A. Khokhlova, O.A. Sapozhnikov, A.A. Naumenko, M.A. Lugovaya, S.A. Shcherbinin, in *Advanced Nano- and Piezoelectric Materials and Their Applications*, Chap. 23, eds. by I.A. Parinov (Nova Science Publishers Inc., New York, 393 (2014)
18. A. Sarvazyan, L.A. Ostrovsky, A. Rybyanets, *AIP Conf. Proc.* **6**, 020002 (2009)
19. A.N. Rybyanets, *Ferroelectrics* **419**, 90 (2011)
20. A. Rybianets, A.V. Nasedkin, *Ferroelectrics* **360**, 57 (2007)
21. A.N. Rybyanets, A.A. Naumenko, N.A. Shvetsova, in *Nano- and Piezoelectric Technologies, Materials and Devices*, Chap. 1, eds. by I.A. Parinov (Nova Science Publishers Inc., New York, 2013), p. 275